

Density measurement through elastic electron scattering with a gaseous target at the Jefferson Lab *

ZHANG Yi(张毅)¹ QIAN Xin(钱鑫)² HU Bi-Tao(胡碧涛)^{1;1)}

¹ School of Nuclear Science and Technology, Lanzhou University, Lanzhou 730000, China

² Kellogg Radiation Laboratory, California Institute of Technology, CA 91125, US

Abstract: We report the density measurement through e-³He elastic scattering with a 1.23 GeV electron beam in Jefferson Lab experiment E06-010. The extracted ³He density is (9.26±0.06) amagats and the N₂/³He ratio is (1.49±0.08)%. In addition, these results are consistent with the deduced target densities based on pressure broadening measurement.

Key words: pressure curve, dilution, polarized ³He target, elastic scattering, radiative correction

PACS: 25.30.Bf, 13.40.Ks **DOI:** 10.1088/1674-1137/36/7/008

1 Introduction

Semi-inclusive deep inelastic scattering (SIDIS) of leptons, where the scattered lepton and one of the leading hadrons produced in the final state are detected in coincidence, plays an important role in accessing transverse momentum dependent parton distribution functions (TMD), which describe the nucleon structure in 3-D momentum space. These TMDs reveal important information about the nucleon structure and QCD dynamics.

In Jefferson Lab Hall-A, the first measurement of target transverse single-spin asymmetry (SSA) on a neutron was performed through SIDIS. The Collins/Sivers moments are reported in [1, 2]. Since there is no stable free neutron target in nature, polarized ³He was used as an effective polarized neutron target. This is based on the fact that the ground state of ³He is dominated by *S* state [3], where the two protons are anti-parallel to each other, and the polarized neutron contributes to all the spins of ³He.

In order to obtain the measurement of a neutron by measuring ³He, one has to correct the yield contributions of the two protons. In practice, data were taken on a reference target filled with known amounts of hydrogen gas (free proton) at the same kinematics as ³He data. In addition, one has to know the den-

sity of ³He gas in order to properly correct the proton dilution. In this paper, we present the results of target density analysis with elastic e-³He scattering and compare with the model calculated density which is based on the averaged target density from pressure broadening measurement.

In the deeply inelastic lepton scattering experiment, the core part of a polarized ³He target is a glass cell, which contains the ³He gas. The glass cell (also referred to as the production cell) of the polarized ³He target has a 2-chamber structure, as shown in Fig. 1. In the top chamber (also referred to as the pumping chamber), the ³He gas was polarized by spin exchange optical pumping (SEOP) [4]. The polarized ³He nuclei diffused to the bottom chamber (also referred to as the target chamber), where the electron beam was passing through (shown as the dashed line in Fig. 1).

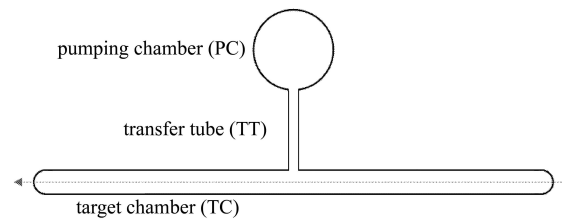


Fig. 1. Schematic view of the ³He glass cell.

Received 10 October 2011

* Supported by National Natural Science Foundation of China (11075068, 10775062, 91026021, 11135002)

1) E-mail: hubt@lzu.edu.cn

©2012 Chinese Physical Society and the Institute of High Energy Physics of the Chinese Academy of Sciences and the Institute of Modern Physics of the Chinese Academy of Sciences and IOP Publishing Ltd

During SEOP, the pumping chamber was required to be heated to about 250 °C, while the typical temperature of the target chamber was in a range between 40 °C to 120 °C. Such a large temperature difference led to a nonuniform density distribution of the gas inside the cell. On the other hand, the average density over the 2 chambers at the same temperature was accessed by measuring the pressure broadening of the absorption spectrum of the Alkali atom [5]. Therefore, the effective average density in the target chamber can be deduced from the average target density and a model calculation can be made based on the temperature measurement with resistive thermal devices (RTD). In order to evaluate the systematic uncertainties introduced by the temperature model, it is important to provide an independent measurement of effective density in the target chamber. In addition, a small amount of N₂ gas was also injected into the cell to maintain the polarization of ³He. The injected nitrogen also led to a yield which diluted the yield of polarized ³He gas in the measurement of SSA. Therefore, it is also crucial to confirm the density ratio of N₂ to ³He.

During the experiment, data were taken on a reference cell filled with various known amounts of ³He gas and nitrogen gas. The left high resolution spectrometer (HRS_L) [6] was set at the elastic kinematics to detect the elastically scattered electrons. The measured yields of the electron elastic scattering on the reference cell were then compared with those on the production cell in order to evaluate the density of the gas in the production cell. Various corrections, including single-track efficiency, radiative correction, cell wall contamination, etc. were also taken into account in this analysis.

2 Yield extraction

The raw data were firstly skimmed following the standard data quality check procedure [7], in which the beam trip and the periods with instrumental issues were removed. In order to select good events, a standard HRS_L acceptance cut [8], an electron identification cut and a vertex Z cut (shown in Fig. 2)¹⁾ were used.

Then the beam charge, Q , which is read from the beam charge monitor, and the computer live time T_t ,

defined as

$$T_t = \frac{N_{\text{hrs}}}{S_{\text{hrs}} - S_{\text{edtp}}}, \quad (1)$$

are calculated. Here, N_{hrs} stands for the number of HRS_L events, S_{hrs} stands for the scaler counts of HRS_L and S_{edtp} stands for the scaler counts of manually generated pulses to measure the electronics dead time.

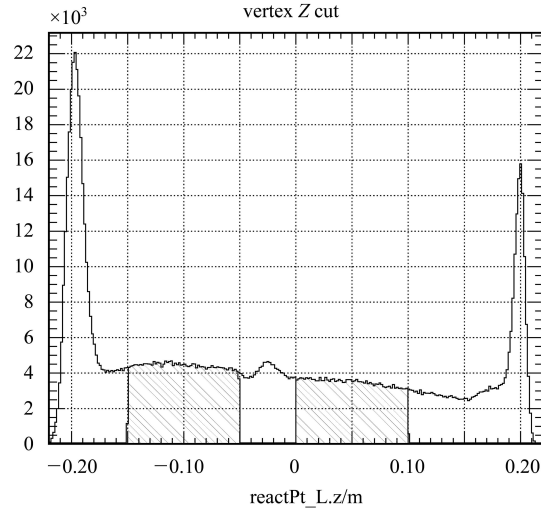


Fig. 2. Vertex Z cut for the production cell. Only the shadowed regions are selected.

In order to identify e-³He and the e-N events, the cuts on missing mass²⁾ are defined separately, as shown in Fig. 3 and Fig. 4, respectively. In the nitrogen case, we also include the first excitation peak which is composed of the contributions from several excited states of the ¹⁴N nuclei [9] to increase the statistics.

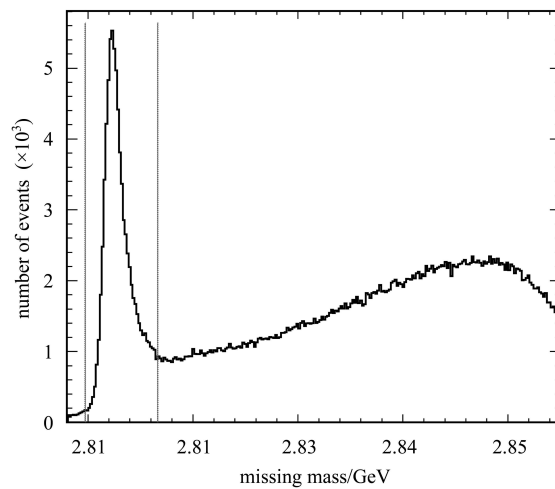


Fig. 3. The ³He missing mass spectrum.

1) In this work we chose the range as $[-15, -5] \cup [0, 10]$ cm in order to exclude the contamination of the glass cell window and to exclude the range $([-5, 0]$ cm) where the wall thickness of the glass cell was not uniform, as shown in Fig. 2.

2) Here the missing mass is defined as the amplitude of a 4-D momentum which is “missed” by the detector and is equal to the momentum of an incident electron plus the momentum of the target nuclei minus the momentum of a scattered electron.

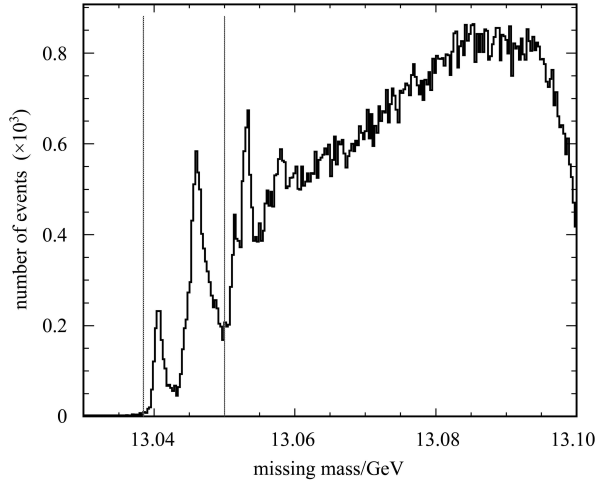


Fig. 4. The nitrogen missing mass spectrum.

The extracted yields are then defined as:

$$Y_{3\text{He}}^{\text{raw}} = \frac{N_{3\text{He}}}{Q \cdot T_t \cdot E_{\text{single-track}}}, \quad (2)$$

$$Y_{3\text{He}} = Y_{3\text{He}}^{\text{raw}} \cdot \left(1 - R_{\text{N}/3\text{He}} \cdot \frac{\rho_{\text{N}_2}}{\rho_{3\text{He}}}\right), \quad (3)$$

$$Y_{\text{N}} = \frac{N_{\text{N}}}{Q \cdot T_t \cdot E_{\text{single-track}}}. \quad (4)$$

Here $N_{3\text{He}(\text{N})}$ stands for the number of good elastic events from helium-3 (or nitrogen) after all cuts. The $R_{\text{N}/3\text{He}}$ term represents the contamination from the N_2 to ^3He . $E_{\text{single-track}}$, which is defined as the ratio of number events with only 1 track to that of events with tracks:

$$E_{\text{single-track}} = \frac{N_{1\text{ track}}}{N_{\text{tracks}}}, \quad (5)$$

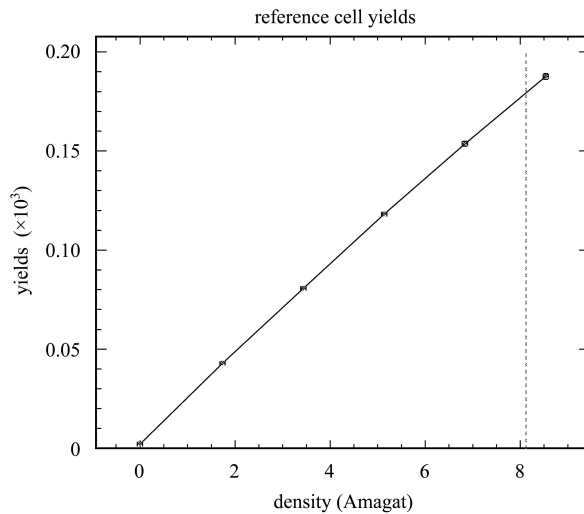


Fig. 5. Yield vs density for the reference cell ^3He runs. The dashed line shows where the filling density of the production cell is.

is the single track efficiency, since we require only the good event, it contains one track. Then we extract the yields of the reference cell ^3He runs as shown in Fig. 5.

3 Radiative correction

To compare the yields from the reference cell to those from the production cell, the effect of radiative correction [10] needs to be taken into account, since the thicker wall of a cell leads to a larger energy loss and consequently further shifts and broadens the elastic peak in the missing mass spectrum. In addition, since the temperature distributions in the reference cell and production cell are different, a vertex-position-dependent correction is also applied. Both corrections are performed by using a Monte-Carlo simulation.

The simulation program used is SAMC [11]. The average A (average number of nucleons), Z (average number of proton), and effective radiation length for incident and scattered electrons are updated.

Figure 6 shows a comparison of the missing mass spectrum of the simulation (red) and that of the data (black). Here the simulation has been scaled to the data for comparison. The applied elastic cut is selecting the region between the two solid lines. In order to properly model the detector resolution in the missing mass spectrum, an additional smearing of 480 keV

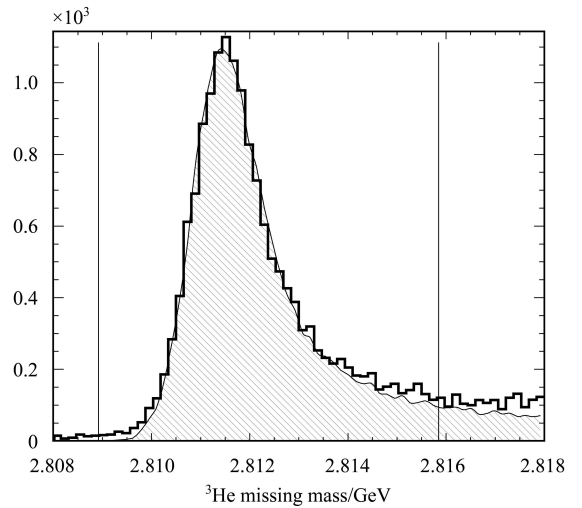


Fig. 6. The ^3He missing mass spectrum of the simulation (shaded area) and the data. The simulation has been smeared by 480 keV. In the data there are some contributions from the inelastic $e\text{-}^3\text{He}$ scattering, while in the simulation only elastic scattering is taken into account.

is directly applied, which is consistent with the measured detector resolution from the HRS optics calibration.

In the simulation, the events are uniformly generated through the entire target length. However, this is not the case in the experiment due to the nonuniform temperature distribution as shown in Fig. 7. In order to coherently consider this effect with the nonuniform acceptance, when calculating the yield in simulation, each simulated event is weighted by the density ratio of the calculated density to the average density ($\rho(z)/\bar{\rho}$), which is extracted from the measured target chamber temperatures. Here, $\bar{\rho}$ is calculated as:

$$\bar{\rho} = \frac{\int \rho(z) dz}{\int dz}. \quad (6)$$

This correction leads to a reduction of about 0.3% on the yield of the simulation for the production cell, while it is negligible for the reference cell due to a much more uniform temperature distribution.

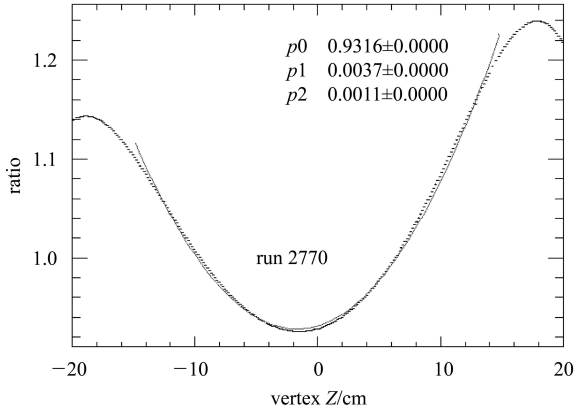


Fig. 7. Vertex dependence of the density due to the temperature distribution. The solid curve is a second order polynomial fit.

4 Pressure curve

In the pressure curve analysis, the yield of the reference cell need to be converted to that of the production cell by using the following formula:

$$Y_{\text{prod}}^{\text{ref}} = (Y_{\text{ref}}^{\text{data}} - Y_{\text{ref}}^{\text{empty}}) \cdot \frac{Y_{\text{prod}}^{\text{MC}}}{Y_{\text{ref}}^{\text{MC}}} + Y_{\text{ref}}^{\text{empty}}. \quad (7)$$

Here $Y_{\text{ref}}^{\text{data}}$ is the yield in Eq. (2) and Eq. (4) extracted from the reference cell data. $Y_{\text{ref}}^{\text{empty}}$ is the yield of a reference cell run in which the reference cell was vacuumized. $Y_{\text{prod}}^{\text{MC}}/Y_{\text{ref}}^{\text{MC}}$ takes into account the radiative correction and the vertex dependent density correction from simulation, as discussed in the previous section. The typical value is about 17%.

In addition, it is more useful to plot yield vs. density than yield vs. pressure to exclude the effects induced by temperature.

The results of the ^3He density curve and the N_2 density curve are shown in Fig. 8 and Fig. 9, respectively. The results are fitted with linear functions. Due to the tiny amount of nitrogen in the production cell and the relative smallness of the nitrogen elastic cross section, there are only limited elastic events. So we also include the events from the first excitation peak of nitrogen to calculate the yield. However, the simulation can only precisely calculate the elastic cross section. Thus for the nitrogen density curve, the radiative correction is treated as the one of ^3He , which has been explicitly calculated through the Monte-Carlo simulation in Sec. 3, since the ratio is dominated by the difference of wall thicknesses

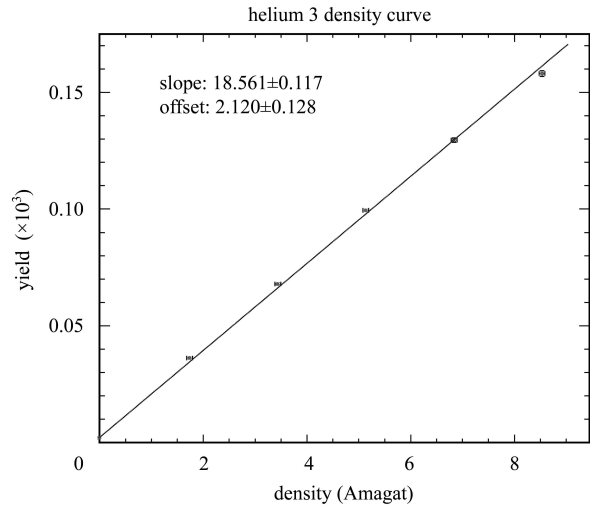


Fig. 8. The density curve of reference cell ^3He runs, fitted with a linear function.

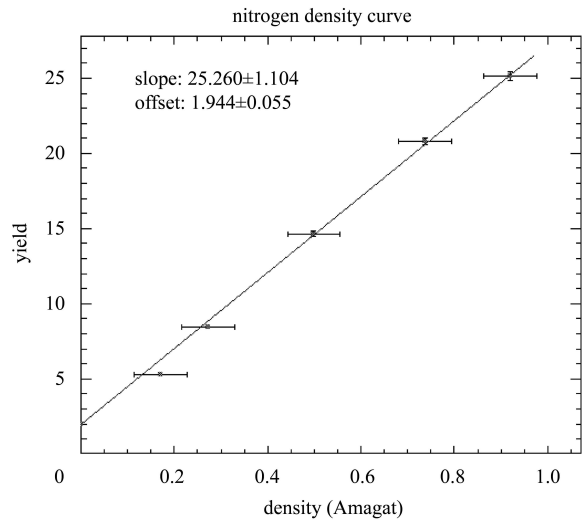


Fig. 9. The density curve of reference cell nitrogen runs, fitted with a linear function.

between the production cell and the reference cell. A dedicated check of comparing the simulated elastic nitrogen yields of the reference cell and of the production cell confirms this.

5 N₂ contamination

As the nitrogen nucleus is heavier than the ³He nucleus, the elastically scattered electrons from nitrogen carry higher energies than those from ³He. Therefore, the in-elastically scattered electrons from nitrogen nuclei can contaminate the ³He elastic peak in Fig. 3. In Eq. (3), $R_{N/{}^3\text{He}} \cdot \rho_{N_2} / \rho_{{}^3\text{He}}$ represents this contamination. $R_{N/{}^3\text{He}}$ is the contamination ratio of N₂ in the ³He elastic yield when the amounts of N₂ and ³He are the same. Then the density ratio $\rho_{N_2} / \rho_{{}^3\text{He}}$ scales the contamination ratio to the case of production cell. The factor $R_{N/{}^3\text{He}}$ can be determined by the nitrogen reference cell data after applying the ³He elastic cut. Fig. 10 shows the yield vs. density of nitrogen on the reference cell runs after applying the ³He elastic cut. Compared with those on the reference cell ³He runs (shown as Fig. 5), the central value of the ratio $R_{N/{}^3\text{He}}$ is 1.38, while its uncertainty is determined to be 0.06.

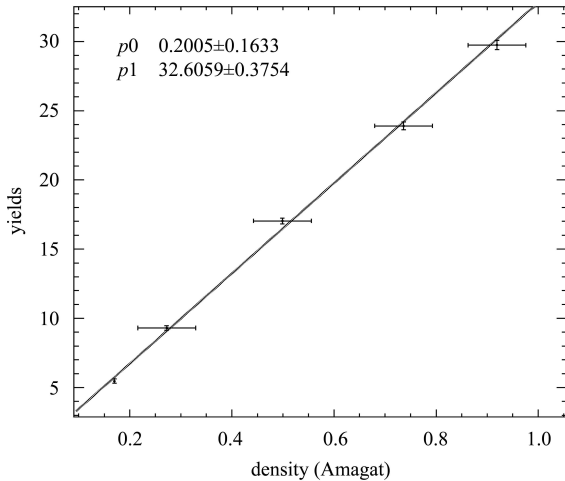


Fig. 10. The yields of reference cell nitrogen runs with ³He cuts are fitted as a linear function.

6 Results and uncertainties

As presented in Fig. 9, the nitrogen density curve data are fitted with a linear function. For each point, the uncertainty on x -axis is from the systematic uncertainty of pressure gauge installed on the reference cell, which is estimated as 1 psi for both gases. The uncertainty of the y -axis is the statistic uncertainty

of the yield for each data point. The same fit is also performed for the ³He density curve. However, since the densities of ³He are much larger than the nitrogen ones, the error bars are difficult to see.

To obtain the nitrogen density in the production cell, it is necessary to estimate the backgrounds of the yield in the production cell runs properly. From the wall and window thickness measurement, it is known that the averaged thickness of the production cell windows is 95% of the reference cell one. So the backgrounds coming from the two cells' windows are reasonably assumed to follow the same scale. The density of the nitrogen in the production cell can be written as:

$$\rho_N^{\text{prod.}} = \frac{Y_N^{\text{prod.}} - 0.95 \cdot Bkg_N^{\text{ref.}}}{K_N^{\text{ref.}}} \quad (8)$$

From Eq. (8) the density of nitrogen in the production cell is known as (0.138 ± 0.007) amagats.

For the ³He case, the equation for ³He can be written as

$$\rho_{\text{he}}^{\text{prod.}} = \frac{(Y_{\text{he}}^{\text{prod.}} - 0.95 \cdot Bkg_{\text{he}}^{\text{ref.}}) \times (1 - R_{N/{}^3\text{He}} \cdot \rho_N^{\text{prod.}} / \rho_{\text{he}}^{\text{prod.}})}{K_{\text{he}}^{\text{ref.}}} \quad (9)$$

From Fig. 8 the slope and the background of the ³He density curve are extracted as (18.65 ± 0.12) and (2.12 ± 0.13) , respectively. The ratio $R_{N/{}^3\text{He}}$ has been defined in Eq. (3) and is known as (1.38 ± 0.06) in Sec. 6. With the density of nitrogen in the production cell, Eq. (9) becomes a 2 order polynomial equation with $\rho_{\text{he}}^{\text{prod.}}$ as the only unknown variable. The density of the ³He in the production cell is then determined to be (9.26 ± 0.06) amagats.

Another test of the method of applying the radiative correction is also performed to study the systematic uncertainties. In this test the radiative correction is applied without subtracting the yield of the reference empty cell run. In this case the slope of the curve is 18.59 and the offset is 2.12. Then the determined ³He density is 9.29 amagats, which is consistent with the previous result.

7 Comparison with pressure broadening measurement

Pressure broadening [12] is a general phenomenon that the line width of an atomic transition line increases linearly with the density of the buffer gas. Romalis [5] did extensive studies on experiments to

apply this method to polarized ^3He targets. In Experiment E06-010, in order to independently check the target density measured by elastic scattering, we measured the absorption spectrum of the D1 line¹⁾ from Rb atom (as shown in Fig. 11).

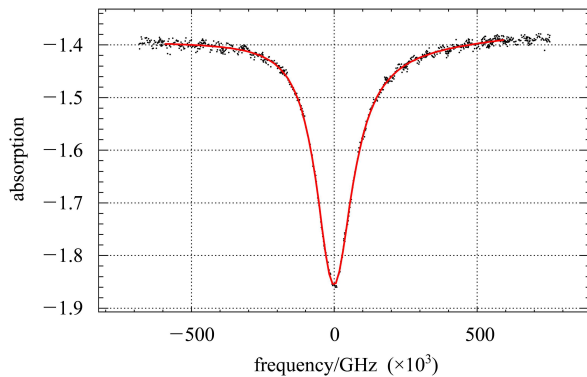


Fig. 11. The absorption spectrum of Rb D1 light.

The production cell used in this work is called “Astralweek”, which was filled with 8.082 amagats

^3He at the University of Virginia [13]. Including the nitrogen density, from the pressure broadening measurement we obtained an average density as large as (8.12 ± 0.10) amagats. Based on this number, and taking the nonuniform temperature distribution into account, the result from the model calculation gives (9.31 ± 0.12) amagats while the elastic data gives (9.40 ± 0.06) amagats for the sum of ^3He and N_2 gas.

8 Conclusion

In this paper we present the analysis of the elastic data in the transversity experiment at the Jefferson Lab. The target densities of both ^3He and nitrogen are obtained and the total density is consistent with the result from the pressure broadening measurement. This work serves as an important step in calculating the nitrogen and proton dilution factors in extracting neutron asymmetries from the measured ^3He asymmetries.

References

- 1 Vincenzo Barone, Alessandro Drago, Philip G. Ratcliffe Phys. Rep., 2002, **359**: 1
- 2 QIAN X et al. Phys. Rev. Lett., 2011, **107**: 072003
- 3 Friar J L, Gibson B F, Payne G L, Bernstein A M, Chupp T E. Phys. Rev. C, 1990, **42**: 23102314
- 4 Walker T G, Happer W. Rev. Mod. Phys., 1997, **69**: 629
- 5 Romalis M V, Miron E, Cates G D. Phys. Rev. A, 1997, **56**: 4569
- 6 Alcorn J et al. Nucl. Instrum. Methods in Phys. A, 2004, **522**: 294
- 7 QIAN X. Ph.D. thesis “Measurement of Single Spin Asymmetry in $n^\uparrow(e, e'\pi^\pm)X$ on Transversely Polarized ^3He ”. http://www.tunl.duke.edu/mep/thesis/Qian_dissertation.pdf (2010)
- 8 <https://hallaweb.jlab.org/dvcslog//transversity/208>
- 9 Ensslin N, Bertozzi W, Kowalski S, Sargent C P, Turchinetz W, Williamson C F, Fivozinsky S P, Lightbody J W, Penner S. Phys. Rev. C, 1974, **9**: 1705–1717
- 10 Tsai Yung-Su. Rev. Mod. Phys., 1974, **46**: 851
- 11 Deur A. Technical note 33 in E94-010 “Single Arm Monte Carlo for Polarized ^3He Experiments in Hall A”. http://www.jlab.org/e94010/tech_note_33.ps.gz
- 12 Nicole Allard, John Keilkopf. Rev. Mod. Phys., 1982, **54**: 4
- 13 Web page of all production cells’ information in University of Virginia. <http://galileo.phys.virginia.edu/research/groups/spinphysics/>

1) The transition from the $5^2S_{1/2}$ state to the $5^2P_{1/2}$ state.